Int. J. Solids Structures, 1971, Vol. 7, pp. 1305 to 1316. Pergamon Press. Printed in Great Britain

INSTABILITY OF STOCHASTICALLY LOADED SHALLOW ARCHES IN NONSYMMETRIC MODES

T. S. SANKAR†

Department of Mechanical Engineering, Sir George Williams University, Montreal, Canada

and

S. T. ARIARATNAM‡

Department of Civil Engineering, University of Waterloo, Waterloo, Canada

Abstract—The problem of stability of shallow, two-pinned, sinusoidal arches subjected to a randomly varying symmetrically distributed lateral loading is investigated. Though the deformation of the arch is initially symmetric, buckling is initiated when an antisymmetric mode is picked up at a certain critical value of the loading. Based on an analysis previously developed by the authors for asymmetric snap-buckling cases applicable to shell problems, analytical expressions are derived for calculating the probability of first snapping of the arch in a specified time interval from an initial stable equilibrium state. Numerical results for a particular example of an arch specimen are presented and discussed.

INTRODUCTION

SNAP-THROUGH and snap-buckling types of instabilities of slender shallow arches have been extensively investigated in recent years. Such phenomena involve the structure leaving an initial stable equilibrium configuration for another nonadjacent stable equilibrium state undergoing large displacements and are characterized by a finite jump over a potential energy barrier at certain critical loading conditions. When the loading is time-dependent, the behaviour of the arch is analogous to the "jump phenomenon" in the theory of nonlinear vibrations and has been investigated by Mettler [1], Hoff and Bruce [2], Lock [3], Humphreys [4], Hsu [5, 6], etc., all of whom considered different shapes of arches under different types of deterministic lateral loads. Corresponding studies of the problem when the loading varies randomly have been very few.

If the initial central rise of the arch is small, the deformation is entirely in a single, symmetric mode when subjected to a symmetrically distributed dynamic load and the arch loses its stability by what is known as a symmetric snap-through. Here, the analysis essentially involves a discussion of the motion of an equivalent point mass on the potential energy surface which has a single maximum corresponding to an unstable equilibrium configuration of the arch. In a previous paper, the present authors [7] considered a similar problem when the loading is stochastic and derived the probability of first snap-through of the arch in a specified time. Their approach involved the determination of the rate of diffusion of the probability density across the potential hump in the direction of the

† Associate Professor.
‡ Professor.

symmetric mode in the phase plane and was based, in part, on a theory proposed by Kramers [8] in his paper on the kinetics of chemical reactions. When the initial central height of the arch exceeds a certain limiting value, along with the fundamental symmetric mode of deformation, the next antisymmetric mode is also excited at the onset of buckling even though the loading is symmetrical. Such an instability may be termed as "snap-buckling" to distinguish it from the symmetric snap-through case mentioned above. Here, an unstable equilibrium state of the arch is represented by a saddle point on the potential energy surface and the motion of the system under small dynamic disturbances will follow a path for which the slope of descent is everywhere a maximum. The authors [9] have presented a general treatment of such snap-buckling problems for shell-type structures subjected to random loading. Their analysis technique involves the estimation of a slow diffusion rate of the probability density along the above-mentioned path of steepest descent which also coincides with one of the principal curvature directions of the potential energy surface.

The problem of asymmetric dynamic instability of shallow arches that is considered in the present paper is an extension of the analysis given in the previous paper [9] by the authors. In order to make this presentation reasonably self-explanatory, some important ideas of the theory in the earlier paper [9] are explained within the context of the present problem. For simplicity, both the shape of the arch and the lateral load distribution are assumed to be sinusoidal and only the fundamental symmetric mode and the fundamental antisymmetric mode of deformations are considered.

FORMULATION OF THE PROBLEM

Consider a shallow, two-pinned, sinusoidal arch rib whose initial central rise w_0 is chosen such that, along with a symmetric deformation, an antisymmetric deformation is also excited under the action of the given loads. With the coordinate axes as indicated in Fig. 1, the undeformed shape of the centreline of the arch is given by

$$w_0(x) = y_0 \sin\left(\frac{\pi x}{l}\right), \tag{1}$$

where l is the span. Let the arch be initially in a stable equilibrium configuration under a symmetrically distributed deterministic load of intensity $W \sin(\pi x/l)$. At time $t = 0$, let the arch be subjected to a random load of intensity $f(t)\sin(\pi x/l)$ having a zero mean value. Because of the assumption that the arch has two degrees of freedom, the deformed shape of the centreline of the rib at any instant will be given by

$$w_1(x, t) = \sum_{n=1}^{2} y_n(t) \sin\left(\frac{n\pi x}{l}\right).$$

The deflection of the crown is then

$$q_1 = y_0 - y_1(t),$$

and at any other arbitrary point the deformation as measured from the crown is

$$\begin{aligned} w(x, t) &= w_0(x) - w_1(x, t), \\ &= q_1 \sin\left(\frac{\pi x}{l}\right) - q_2 \sin\left(\frac{2\pi x}{l}\right). \end{aligned} \tag{2}$$

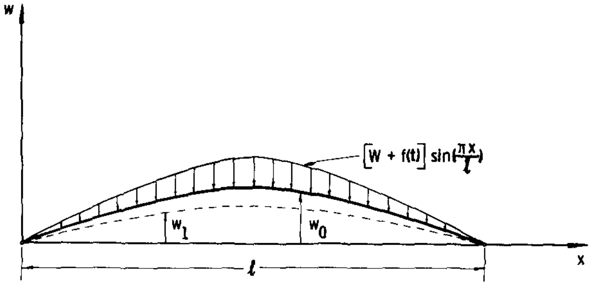

FIG. 1. Geometry of the arch.

Taking the coefficient of viscous damping β_0 to be the same in both q_1 and q_2 modes of deformation, the equations of motion of the arch may be written using Lagrange's equations

$$\frac{\mathrm{d}}{\mathrm{d}t}\left(\frac{\partial T}{\partial \dot{q}_i}\right)+\frac{\partial D}{\partial \dot{q}_i}-\frac{\partial T}{\partial q_i}+\frac{\partial V}{\partial q_i} = Q_i, \tag{3}$$

where the index i takes the values 1 and 2, T is the kinetic energy of the system, D the dissipation function, V the potential energy and Q_i the generalized forces corresponding to the applied loading on the arch. The quantities T, D and Q_i are evaluated as follows

$$T = \tfrac{1}{4}ml(\dot{q}_1^2+\dot{q}_2^2),$$
$$D = \tfrac{1}{4}\beta_0 l(\dot{q}_1^2+\dot{q}_2^2),$$
$$Q_1 = \tfrac{1}{4}lf(t), Q_2 = 0,$$

where m is the mass of the arch per unit length. The potential energy V of the arch is determined from the strain energy V_a due to axial shortening, the strain energy V_b due to bending and the work done V_w by the external dead load $W\sin(\pi x/l)$. That is

$$\begin{aligned} V(q_1, q_2, \lambda) &= V_a+V_b-V_w \\ &= \frac{Kl}{8r^2}\{[\tfrac{1}{2}q_1(2y_0-q_1)-2q_2^2]^2 \\ &\quad +2r^2q_1^2+32q_2^2-8\lambda r^3 q_1\}+\text{const.}, \end{aligned} \tag{4}$$

where r is the radius of gyration of the section of the arch, A the area of cross section, E the Young's modulus, $K = EA\pi^4r^2/l^4$ and the dead load parameter $\lambda = Wl^4/2\pi^4EAr^3$. Substitution of the above expressions in equation (3) yields the following equations of motion

$$\begin{aligned} \ddot{q}_1+\beta\dot{q}_1+\frac{\partial V}{\partial q_1} &= \xi(t), \\ \ddot{q}_2+\beta\dot{q}_2+\frac{\partial V}{\partial q_2} &= 0, \end{aligned} \tag{5}$$

where

$$\frac{\partial V}{\partial q_1} = \frac{-K}{4r^2 m}[q_1^3 - 3y_0 q_1^2 + q_1(2y_0^2 + 4r^2) + 4q_1 q_2^2 - 4y_0 q_2^2 - 8\lambda r^3], \tag{6}$$

$$\frac{\partial V}{\partial q_2} = \frac{-K}{r^2 m}(q_1^2 q_2 - 2y_0 q_1 q_2 + 16r^2 q_2 + q_2^3), \tag{7}$$

$$\beta = \frac{\beta_0}{m} \text{ and } \xi(t) = \frac{1}{m} f(t).$$

The equilibrium configurations of the arch for any given value of the static load parameter λ are given by

$$\frac{\partial V}{\partial q_1} = 0, \qquad \frac{\partial V}{\partial q_2} = 0,$$

and on using expressions (6) and (7), these equilibrium equations become

$$q_1^3 - 3y_0 q_1^2 + q_1(2y_0^2 + 4r^2) + 4q_1 q_2^2 - 4y_0 q_2^2 - 8\lambda r^3 = 0, \tag{8}$$

$$q_1^2 q_2 - 2y_0 q_1 q_2 + 16r^2 q_2 + q_2^3 = 0. \tag{9}$$

The roots of these equations describe the load–deflection characteristics of the arch as shown in Fig. 2. Let λ_{max} and λ_{min} be the upper and lower static buckling loads of the arch. Then, for any value of λ satisfying the inequality $\lambda_{min} < \lambda < \lambda_{max}$, it may be seen that there exist four equilibrium configurations for the arch corresponding to the points A, B, B_1 and C in Fig. 2. The contours of equal potential energy values are indicated in Fig. 3, where the equilibrium states of the structure for any λ may be seen to be located at the bottom of "depressions", the top of "hills" and at "saddle points". The initial stable state A and the final buckled state C of the arch are associated with the symmetric deformation mode q_1 only and are located at the bottom of the valleys since they are associated with a minimum of the potential energy. The unstable equilibrium configuration B_1 is also associated only with the symmetric deformation q_1 (with $q_2 = 0$) describing symmetric snap-through type of problems [7] and is located at the top of a hill to represent a maximum of the potential energy. The other unstable equilibrium configuration B of the structure, which is of interest

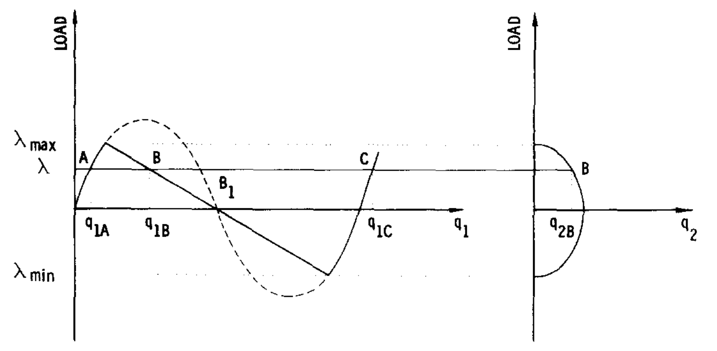

FIG. 2. Load–deflection curves for the arch.

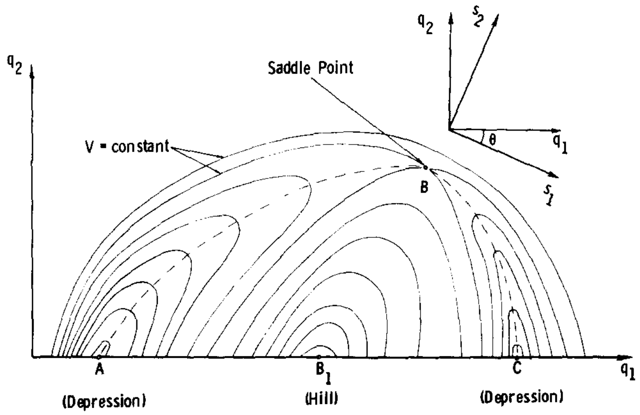

FIG. 3. Contours of equal potential energy.

in this paper, is associated with both symmetric and antisymmetric deformations and hence is located at a saddle point on the potential energy surface. The equilibrium configurations corresponding to $A(q_1 = q_{1A}, q_2 = 0)$ and $C(q_1 = q_{1C}, q_2 = 0)$ are given by the roots of the equation (8) after setting $q_2 = 0$ and that of $B(q_1 = q_{1B}, q_2 = q_{2B})$ is given by a solution satisfying both the equations (8) and (9).

When the stochastic load $\xi(t)$ is applied, the dynamic state of the arch at any subsequent time will be described by the phase variables $(q_1, q_2, \dot{q}_1, \dot{q}_2)$. For different members of the loading $\xi(t)$, there will be an ensemble of random trajectories of the phase point starting from the initial stable equilibrium state A. After a specified time T, some of these trajectories may have remained entirely within the neighbourhood of A while some others may have surmounted the potential barrier and crossed over to the buckled state C. Since the potential energy level at B_1 is higher than that at B, it may be expected that the phase trajectories crossing over to C will be concentrated in the vicinity of the equilibrium point B. The problem is to determine the probability P_T that in a time interval T the arch would have snapped and be found in the neighbourhood of C. If the rate of flux j_B of the phase trajectories across a certain boundary perpendicular to their paths in the neighbourhood of B can be determined [9], then the probability P_T will be given by the number of phase trajectories crossing over to C in a time T divided by the number n_A of the trajectories that were originally in the neighbourhood of the initial stable state A. Explicitly stated,

$$P_T = \frac{j_B T}{n_A}. \tag{10}$$

The calculation of the flux rate j_B and the quantity n_A requires an exact solution of the stochastic differential equation governing the response probability density satisfying the intitial condition that the arch is in a stable equilibrium A at $t = 0$.

FOKKER–PLANCK EQUATIONS

Given an arbitrary random process $\xi(t)$, the equation governing the response probability is not known. However, if $\xi(t)$ is a stationary, wide-band random excitation with a delta correlation, the response process can be approximated by a Markov process and the Fokker–Planck equation can be used.

Writing the equations of motion (5) as a set of state equations, the Fokker–Planck equation giving the probability of response can be derived to be

$$\frac{\partial p}{\partial t} = \frac{\partial V}{\partial q_1}\frac{\partial p}{\partial \dot{q}_1} - \dot{q}_1\frac{\partial p}{\partial q_1} + \frac{\partial V}{\partial q_2}\frac{\partial p}{\partial \dot{q}_2} - \dot{q}_2\frac{\partial p}{\partial q_2} + \beta\frac{\partial}{\partial \dot{q}_1}\left(\dot{q}_1 p + \frac{D}{\beta}\frac{\partial p}{\partial \dot{q}_1}\right) + \beta\frac{\partial}{\partial \dot{q}_2}(\dot{q}_2 p), \tag{11}$$

where

$$\langle \xi(t_1)\xi(t_2)\rangle = 2D\delta(t_1 - t_2),$$

the angular brackets denoting the ensemble average and D the intensity coefficient. Since the arch is in equilibrium in the configuration ($q_1 = q_{1A}$, $q_2 = 0$) at time $t = 0$, any solution of equation (11) must satisfy the condition

$$p(\dot{q}_1, \dot{q}_2, q_1, q_2, t) \to \delta(q_1 - q_{1A})\delta(q_2)\delta(\dot{q}_1)\delta(\dot{q}_2) \text{ for } t \to 0^+. \tag{12}$$

The exact solution of equation (11) satisfying the initial condition (12) is not known. However, if the energy supplied by the random forces is taken to be small compared to the height of the potential barrier, the equation (11) can be approximately solved. Explicitly stated, this condition is

$$\frac{D}{\beta} \ll h, \text{ where } h = V(q_{1B}, q_{2B}) - V(q_{1A}, 0). \tag{13}$$

Such an assumption will result in a motion of the phase trajectories, starting from the point A, that is slow and almost stationary as explained in a previous paper by the authors [7]. Consequently, the relation time τ for the probability flow in the phase space representing the motion of the phase trajectories will be large. Further, if $T \ll \tau$, the direction of this drift near the region B will be principally towards C and the probability of snapping P_T evaluated will then represent the probability that the arch snaps for the first time. Therefore, the probability density valid in the neighbourhood of any point in the phase space will be that corresponding to the stationary solution of the Fokker–Planck equation (11) with the potential function V appropriate to the neighbourhood of that point. Thus, the probability density in the neighbourhood of A will be the stationary solution of the equation (11) with the antisymmetric deformation $q_2 = 0$ and is given by

$$p_A = \alpha_A \exp\left\{-\frac{\beta}{D}[\tfrac{1}{2}\dot{q}_1^2 + \tfrac{1}{2}(V_{11})_A(q_1 - q_{1A})^2 - h]\right\}. \tag{14}$$

Here, α_A is a normalizing constant and $(V_{11})_A$ is the first non-vanishing term d^2V/dq_1^2 in the expansion of $V(q_1, q_2, \lambda)$ evaluated at the equilibrium point A. The datum for the potential function is chosen such that $V = 0$ at the point B. The solution (14) is to be used to calculate n_A in the formula (10).

Consider those phase trajectories that have succeeded in surmounting the potential barrier at the saddle point B under the shuttling action of the random force $\xi(t)$. The projection of these trajectories on the q_1–q_2 plane will be nearly parallel, around the point B, to the projection of the line of downward curvature of the potential energy surface at B. Let s_1 and s_2 denote the principal curvature coordinates of the potential energy surface and let s_1 correspond to the direction of downward curvature at the point B as indicated in Fig. 3. The transformation law relating the s-system and the original q-system of coordinates is

$$\begin{aligned} q_1 &= s_1 \cos\theta + s_2 \sin\theta, \\ q_2 &= -s_1 \sin\theta + s_2 \cos\theta, \end{aligned} \tag{15}$$

where θ is the angle of transformation. Let V^* be the potential energy of the arch in terms of the new variables s_1 and s_2. $V^*(s_1, s_2, \lambda)$ can be obtained from $V(q_1, q_2, \lambda)$ using equations (15). An advantage of representing the potential function by $V^*(s_1, s_2, \lambda)$ is that, in the expansion, the variations of V^* occur uniquely with respect to each s_1 and s_2 direction and the cross differential terms $\partial^2 V^*/\partial s_i \partial s_j$ vanish for $i \neq j$, whereas this is not true if the potential energy is written in terms of the original q-system of coordinates. Consequently, a solution of the Fokker–Planck equation valid near the point B is made possible. Since the cluster of random phase trajectories near the point B will be essentially directed along the principal s_1-direction towards the point C, the probability of snapping of the arch can be determined from the expression (10) where j_B now represents the rate of flux of the phase points across the surface $s_1 = s_{1B}$ in the phase space. This can be evaluated from a solution of the Fokker–Planck equation that is reformulated in terms of the s-coordinate system.

The equations of motion of the arch (5) as referred to the principal s_1 and s_2 coordinates are

$$\begin{aligned} \ddot{s}_1 + \beta\dot{s}_1 + \frac{\partial V^*}{\partial s_1} &= \xi(t)\cos\theta, \\ \ddot{s}_2 + \beta\dot{s}_2 + \frac{\partial V^*}{\partial s_2} &= \xi(t)\sin\theta. \end{aligned} \tag{16}$$

The corresponding Fokker–Planck equations governing the marginal probability densities $p_1(s_1, \dot{s}_1)$ and $p_2(s_2, \dot{s}_2)$ valid in the neighbourhood of the saddle point B are

$$\frac{\partial p_1}{\partial t} = \frac{\partial V^*}{\partial s_1}\frac{\partial p_1}{\partial \dot{s}_1} - \dot{s}_1\frac{\partial p_1}{\partial \bar{s}_1} + \beta\frac{\partial}{\partial \dot{s}_1}\left(\dot{s}_1 p_1 + \frac{D\cos^2\theta}{\beta}\frac{\partial p_1}{\partial \dot{s}_1}\right), \tag{17}$$

$$\frac{\partial p_2}{\partial t} = \frac{\partial V^*}{\partial s_2}\frac{\partial p_2}{\partial \dot{s}_2} - \dot{s}_2\frac{\partial p_2}{\partial \bar{s}_2} + \beta\frac{\partial}{\partial \dot{s}_2}\left(\dot{s}_2 p_2 + \frac{D\sin^2\theta}{\beta}\frac{\partial p_2}{\partial \dot{s}_2}\right), \tag{18}$$

where

$$\bar{s}_1 = s_1 - s_{1B}, \qquad \bar{s}_2 = s_2 - s_{2B}.$$

The flux rate j_B across the surface $s_1 = s_{1B}$ may then be obtained from the locally stationary probability density $p_1(s_1, \dot{s}_1)$ satisfying the equation (17). That is,

$$j_B = \int_{-\infty}^{\infty} \dot{s}_1 p_1(s_{1B}, \dot{s}_1)\,\mathrm{d}\dot{s}_1, \tag{19}$$

and this may be used in the expression (10) to evaluate the probability distribution P_T.

PROBABILITY OF SNAP-BUCKLING

Following the calculation procedure explained in the authors' previous paper [9], the quantities j_B and n_A may be determined and the probability of first snap-buckling of the arch may be found as

$$P_T = \frac{T}{2\pi}\cos^2\theta\left[\frac{(V_{11})_A}{-(V^*_{11})_B}\right]^{\frac{1}{2}}\left\{\left[\frac{\beta^2}{4}-(V^*_{11})_B\right]^{\frac{1}{2}}-\frac{\beta}{2}\right\}\exp\left(-\frac{\beta h}{D}\right). \tag{20}$$

Here $(V_{11})_A$ is the quantity d^2V/dq_1^2 evaluated at $q_1 = q_{1A}$ and $(V^*_{11})_B$ is the quantity $\partial^2 V^*/\partial s_1^2$ evaluated at the saddle point B where $s_1 = s_{1B}$ and $s_2 = s_{2B}$. These quantities may be calculated from the potential energy expression (4). Introducing the nondimensional parameters $\zeta_1 = q_1/2r$, $\zeta_2 = q_2/2r$ and $\alpha = y_0/2r$, the expression (4) becomes

$$V(\zeta_1, \zeta_2, \lambda) = 2Kr^2l[(\alpha\zeta_1 - \tfrac{1}{2}\zeta_1^2 - 2\zeta_2^2)^2 + \tfrac{1}{2}\zeta_1^2 + 8\zeta_2^2 - \lambda\zeta_1] + \text{const}. \tag{21}$$

On setting $\partial V/\partial\zeta_1 = 0$ and $\partial V/\partial\zeta_2 = 0$, the equilibrium positions ζ_A, ζ_B and ζ_C of the arch are given by the roots of the following equations

$$\begin{aligned}\zeta_1^3 - 3\alpha\zeta_1^2 + (2\alpha^2 + 4\zeta_2^2 + 1)\zeta_1 - 4\alpha\zeta_2^2 + \lambda &= 0,\\ 4\zeta_2^3 + (\zeta_1^2 - 2\alpha\zeta_1 + 4)\zeta_2 &= 0.\end{aligned} \tag{22}$$

For the stable equilibrium configurations A and C of the arch (see Fig. 2), the antisymmetric deformation $\zeta_2 = 0$ and on using the first of the equations (22)

$$\begin{aligned}\zeta_{1A} &= \alpha - 2\left(\frac{\alpha^2-1}{3}\right)^{\frac{1}{2}}\cos\left(\frac{\pi-\psi}{3}\right),\\ \zeta_{1C} &= \alpha + 2\left(\frac{\alpha^2-1}{3}\right)^{\frac{1}{2}}\cos\frac{\psi}{3},\end{aligned} \tag{23}$$

where ψ is the smallest positive angle satisfying

$$\cos\psi = \left(\frac{\alpha-\lambda}{2}\right)\left(\frac{\alpha^2-1}{3}\right)^{-\frac{3}{2}}.$$

The unstable equilibrium configuration B is given by a solution satisfying both the equations in (22) and is found as

$$\begin{aligned}\zeta_{1B} &= \tfrac{1}{3}(4\alpha - \lambda),\\ \zeta_{2B} &= \tfrac{1}{2}(2\alpha\zeta_{1B} - \zeta_{1B}^2 - 4)^{\frac{1}{2}}.\end{aligned} \tag{24}$$

If the quantities given in equations (23) and (24) are to be real and distinct, the mean load λ must be such that

$$\alpha - 3(\alpha^2-4)^{\frac{1}{2}} < \lambda < \alpha + 3(\alpha^2-4)^{\frac{1}{2}}. \tag{25}$$

The expression (21) for the potential function must be multiplied by a factor $2/ml$ when it is to be used in the equations of motion given in the form of equations (5). That is,

$$V(\zeta_1, \zeta_2, \lambda) = 4\omega_1^2 r^2[(\alpha\zeta_1 - \tfrac{1}{2}\zeta_1^2 - 2\zeta_2^2)^2 + \tfrac{1}{2}\zeta_1^2 + 8\zeta_2^2 - \lambda\zeta_1] + \text{const.}, \tag{26}$$

where ω_1 is the natural frequency of the arch for a zero initial curvature in its fundamental mode ζ_1 after setting $\zeta_2 = 0$ and is given by the quantity $(K/m)^{\frac{1}{2}}$.

The quantities $(V_{11})_A$ and $(V^*_{11})_B$ to be used in the formula (20) may now be calculated from expressions (23), (24) and (26).

$$(V_{11})_A = \frac{\mathrm{d}^2 V}{\mathrm{d}\zeta_1^2} \text{ evaluated at } \zeta_1 = \zeta_{1A} \text{ and } \zeta_2 = 0,$$

$$= \omega_1^2(3\zeta_{1A}^2 - 6\alpha\zeta_{1A} + 2\alpha^2 + 1). \tag{27}$$

$$(V^*_{11})_B = \frac{\partial^2 V^*}{\partial \zeta^{*2}_1} \text{ evaluated at the point } \zeta^*_1 = \zeta^*_{1B}$$

$$\text{and } \zeta^*_2 = \zeta^*_{2B} \text{ where } \zeta^*_i = \frac{s_i}{2r}.$$

The latter quantity can be computed using a Mohr's circle transformation corresponding to equations (15). That is

$$(V^*_{11})_B = \frac{(V_{11})_B + (V_{22})_B}{2} - \tfrac{1}{2}\{[(V_{11})_B - (V_{22})_B]^2 + 4(V_{12})_B^2\}^{\frac{1}{2}}, \tag{28}$$

where $(V_{11})_B$, $(V_{22})_B$ and $(V_{12})_B$ are the quantities $\partial^2 V/\partial\zeta_1^2$, $\partial^2 V/\partial\zeta_2^2$ and $\partial^2 V/\partial\zeta_1\partial\zeta_2$ evaluated at the point $\zeta_1 = \zeta_{1B}$ and $\zeta_2 = \zeta_{2B}$. On using expressions (24) and (26) in (28), $(V^*_{11})_B$ may be written in the form

$$(V^*_{11})_B = \omega_1^2[L - (M^2 + N^2)^{\frac{1}{2}}], \tag{29}$$

where

$$L = -3\zeta_{1B}^2 + 6\alpha\zeta_{1B} + \alpha^2 - 17{\cdot}5,$$

$$M = 5\zeta_{1B}^2 - 10\alpha\zeta_{1B} + \alpha^2 + 14{\cdot}5,$$

and

$$N = 4[-\zeta_{1B}^4 + 4\alpha\zeta_{1B}^3 + (5\alpha^2 - 4)\zeta_{1B}^2 + (2\alpha^3 + 8\alpha)\zeta_{1B} - 4\alpha^2]^{\frac{1}{2}}.$$

Substituting expressions (27) and (29) in the formula (20), the probability of first snapping of the arch in a time interval T is

$$P_T = \frac{T}{2\pi}\cos^2\theta\left[\frac{3\zeta_{1A}^2 - 6\alpha\zeta_{1A} + 2\alpha^2 + 1}{-L + (M^2 + N^2)^{\frac{1}{2}}}\right]^{\frac{1}{2}}$$

$$\left[\left\{\frac{\beta^2}{4} - [L - (M^2 + N^2)^{\frac{1}{2}}]\omega_1^2\right\}^{\frac{1}{2}} - \frac{\beta}{2}\right]\exp\left(-\frac{\beta h}{D}\right), \tag{30}$$

where θ is the angle of transformation given in equations (15) and can be obtained from the relation

$$\tan 2\theta = \frac{2(V_{12})_B}{(V_{11})_B - (V_{22})_B} = \frac{N}{M},$$

which corresponds to the Mohr's circle transformation indicated in expression (28). The height h of the potential barrier is

$$h = V(\zeta_{1B}, \zeta_{2B}) - V(\zeta_{1A}, 0)$$

$$= 4\omega_1^2 r^2\{4(\alpha\zeta_{1B} - 1) - \tfrac{3}{2}\zeta_{1B}^2 - \zeta_{1A}^2(\tfrac{1}{2} + \alpha - \tfrac{1}{2}\zeta_{1A}^2) - \lambda(\zeta_{1B} - \zeta_{1A}) - 4\}. \tag{31}$$

Introducing a non-dimensional damping coefficient γ and writing $\beta = 2\gamma\omega_1$, the expression for P_T takes the form

$$P_T = \frac{T\cos^2\theta}{\tau_1}\left[\frac{3\zeta_{1A}^2 - 6\alpha\zeta_{1A} + 2\alpha^2 + 1}{-L + (M^2+N^2)^{\frac{1}{2}}}\right]^{\frac{1}{2}}$$
$$\{[\gamma^2 - L + (M^2+N^2)^{\frac{1}{2}}]^{\frac{1}{2}} - \gamma\}\exp\left(-\frac{2\gamma\omega_1 h}{D}\right) \tag{32}$$

where τ_1 is the period for the fundamental oscillation ω_1.

NUMERICAL RESULTS AND CONCLUSIONS

To illustrate the application of the formula (32), a model arch made of aluminum and having a span of 24 in. and a cross-section $\frac{1}{2}$ in. depth $\times$ 1 in. width is considered. The natural frequency ω_1 of the model arch for zero curvature and in the symmetric ζ_1 mode is evaluated to be 400 rad./sec. The intensity coefficient $2D$ of the stochastic load on the arch is taken as $8\omega_1^3 r^2$ units to be in agreement with the assumption (13) made in the analysis. The probability of first snap-buckling is calculated for different values of the mean load λ that satisfy the condition $\lambda_{min} < \lambda < \lambda_{max}$ where λ_{min} and λ_{max} are the minimum and maximum static critical loads of the arch specimen. The time T for the snapping is taken to be 48 cycles of the oscillation ω_1 or 48 τ_1 seconds, τ_1 being the period of ω_1.

Figure 4 presents the plot of the logarithm of the probability distribution P_T against the load ratio λ/λ_{max} for different values of the damping factor γ/γ_c, where γ_c is the critical damping in the ζ_1 mode. It may be noticed that the probability of snapping is highly sensitive to changes in the mean load λ and the damping factor γ/γ_c. For example, when $\gamma/\gamma_c = 0{\cdot}60$, a 6·5 per cent decrease in the ratio λ/λ_{max} from a value of 0·80 decreases the probability from 0·60 to 0·07. Similarly, when $\lambda/\lambda_{max} = 0{\cdot}80$, a 25 per cent decrease in the damping factor γ/γ_c from a value of 0·8 increases the probability of snapping from 0·11 to 0·60. Such large variations may be attributed to the presence of the term exponential $(-2\gamma\omega_1 h/D)$ in the formula (32). Here, a small variation in λ causes a large change in the height h of the potential barrier and thereby influences a considerable change in the magnitude of the ratio $h/(D/2\gamma\omega_1)$ satisfying the assumption (13). The influence of the

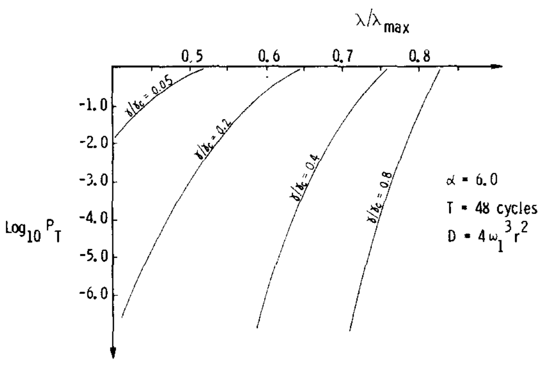

FIG. 4. Probability P_T vs. load ratio λ/λ_{max}.

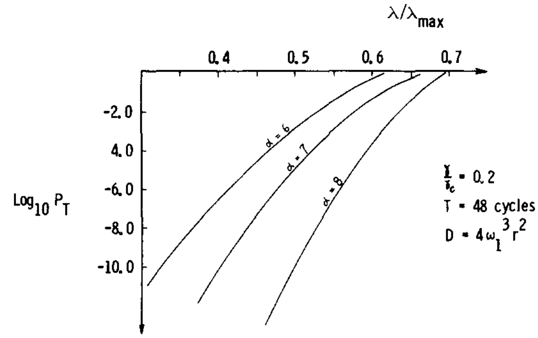

FIG. 5. Probability P_T vs. load ratio λ/λ_{max}.

initial curvature α on the probability of snapping is described by the graphs shown in Fig. 5. As expected, it may be seen that, for the same value of the ratio λ/λ_{max}, the probability P_T decreases for an increase in the initial height α.

The results presented in this paper are applicable to shallow arches that buckle under symmetric and antisymmetric modes of deformation. It is known from static analyses [10] of shallow arches that for such asymmetric snapping to occur the value of the initial curvature parameter α must be greater than $(5\cdot5)^{\frac{1}{2}}$ and therefore the investigation presented here may be taken to be valid in that range of α. For values of α less than $(5\cdot5)^{\frac{1}{2}}$, the arch exhibits only a symmetric mode of deformation and the antisymmetric mode is completely absent. The behaviour of such arches subjected to stochastic loads has been presented in a previous paper [7] and can also be treated as a special case of the results presented in this paper. In such cases, on substituting the asymmetric deformation $\zeta_2 = 0$, the formula (32) for the probability reduces to the one obtained by the authors [7] previously.

It has been often reported that arches and shell structures of its kind, when experimentally tested, always exhibit lower snapping loads than those predicted by the classical theory. The results presented in this paper partly provide an answer to such discrepancies because, besides geometrical imperfections, it may be the small random disturbances (over and above the measured mean static load) caused by the testing machine that have taken the specimen to an eventual snapping. The investigation presented has also an application in the design of structural components of aerospace vehicles, especially in the determination of their reliability against the random aerodynamic forces that are experienced over the dead loads already carried.

Acknowledgement—This work was supported by grants A7104 and A1815 from the National Research Council of Canada.

REFERENCES

[1] E. METTLER, Dynamic Buckling, *Handbook of Engineering Mechanics*, edited by W. FLÜGGE, pp. 62-1–62-11. McGraw-Hill (1962).
[2] N. J. HOFF and V. G. BRUCE, Dynamic analysis of the buckling of laterally loaded flat arches. *J. Math. Phys.* **32**, 276–288 (1953).
[3] M. H. LOCK, The Snapping of a Shallow Sinusoidal Arch Under a Step Pressure Load, Rept. TDR-469 (5240-10)-16, Air Force Systems Command, Los Angeles, Calif. (1965).

[4] J. S. HUMPHREYS, On dynamic snap buckling of shallow arches. *AIAA Jnl* **4**, 878–886 (1966).
[5] C. S. HSU, The effects of various parameters on the dynamic stability of a shallow arch. *J. appl. Mech.* **34**, 349–358 (1967).
[6] C. S. HSU, Stability of shallow arches against snap-through under timewise step loads. *J. appl. Mech.* **35**, 31–39 (1968).
[7] S. T. ARIARATNAM and T. S. SANKAR, Dynamic snap-through of shallow arches under stochastic loads. *AIAA Jnl* **6**, 798–802 (1968).
[8] H. A. KRAMERS, Brownian motion in a field of force and the diffusion model of chemical reactions. *Physica* **7**, 284–304 (1940).
[9] T. S. SANKAR and S. T. ARIARATNAM, Snap-buckling of shell-type structures under stochastic loading. *Int. J. Solids Struct.* **7**, 655–666 (1971).
[10] Y. C. FUNG and A. KAPLAN, Buckling of Low Arches or Curved Beams of Small Curvature, Rept. TN 2840, NACA (1952).

(*Received* 29 *January* 1971)

Абстракт—Исследуется задача устойчивости пологих, защемлённых, синусоидальных арок, подверженных действию безпорядочно переменной, симетрически расположенной, горизонтальной нагрузки. Несмотря на то, что деформация арки сначала симметрическа, выпучивание начинается, когда антисимметрический вид выпучивания появляется при некотором критическом значению нагрузки.

На основе анализа, выведенного раньше авторами для случаев антисимметрического внезапного выпучивания, применяемого для задачи оболочки, определяются аналитические формулы для расчета вероятности пераого прощелкивания, в специфическом интервале времени, от начального устойчивого состояния равновесия. Даются и обсуждаются численные результаты для частного примера образца арки.